CHAPTER 1

Introduction & Literature Survey

1 INTRODUCTION

1.1 Photocatalysis

A photocatalyst absorbs light (UV or visible) energy to drive a reaction. The absorption of energy higher than the bandgap of the material causes the formation of photo-excited electrons and holes. These excited species may then reduce and oxidize adsorbed molecules. Oxidation on the photocatalyst surface quenches the photo-excited holes, while the excited electrons do the reduction part. Thus, light energy absorption by the photocatalyst enables the net transfer of electrons from the oxidized species to the reduced compound. Given the requirement of surmounting a bandgap, conventional photocatalysts always have semiconductor components.

Semiconductor photocatalysis research is now more than a century old. The first photocatalysis experiment was reported by the chemist Giacomo Ciamician in 1901. Later in 1911, the German scientist Alexander Eibner coined the term photocatalysis [Coronodo *et al.* (2013)]. His successful use of ZnO led extensive research on the photocatalytic properties of this semiconductor in subsequent years. Photocatalysis is now seen as a solution for organic pollutant degradation, as a way of harvesting renewable energy sources, and for conducting critical reactions that may not be possible as per the electrochemical series [Weon *et al.* (2019)]. One may say that currently, photocatalysis has pervaded almost all aspects of chemistry.

A semiconducting photocatalyst could be a molecule, a polymer or a crystalline solid material. In case the photocatalyst is soluble in the reaction phase, then it is called a homogeneous photocatalysis process. Otherwise, when the catalyst is a solid dispersed in a liquid phase reaction system, then it is a heterogeneous photocatalyst.

The present thesis work is on heterogeneous photocatalysis and hence, the discussion hereafter is about such photocatalysts only.

1.2 Heterogeneous Semiconductor Photocatalysts

As mentioned earlier, any semiconductor with a bandgap in the UV-visible range can act a photocatalyst. Reaction specific properties of photocatalysts depend on various factors besides its bandgap. The initial research on photocatalysis mainly used pure semiconducting solid particulates. These included various metal oxides, nitrides, chalcogenides etc. [Reber *et al.* (1984), Fujishima *et al.* (2000), Yin *et al.* (2001), Wang *et al.* (2009)]. The next sub-section discusses the basics of the mechanism of action of such a semiconductor photocatalyst.

1.2.1 Mechanism of Semiconductor Photocatalysts

The following steps represent the generally accepted mechanism of semiconductor photocatalysis (figure 1.1).

(i) Light Absorption: In this step, photons get absorbed by the semiconductor, and electron-hole pairs are generated. For light absorption, the energy of the photon should be greater than the bandgap of the semiconductor. Electrons are excited to the conduction band (CB) of the semiconductor, whereas the holes remain in the valence band (VB).

(ii) Recombination: There is also a possibility of electron-hole pair recombination. The recombination may be non-radiative recombination (in the form of heat) or radiative recombination (light emission).

(iii) Separation of excited charges: The electron-hole pairs get separated, and move to the surface of the photocatalyst particles. The long-lived photogenerated charges on the

surface have the potential to promote different redox reactions, based on the donor or acceptor properties of the surface absorbed species.

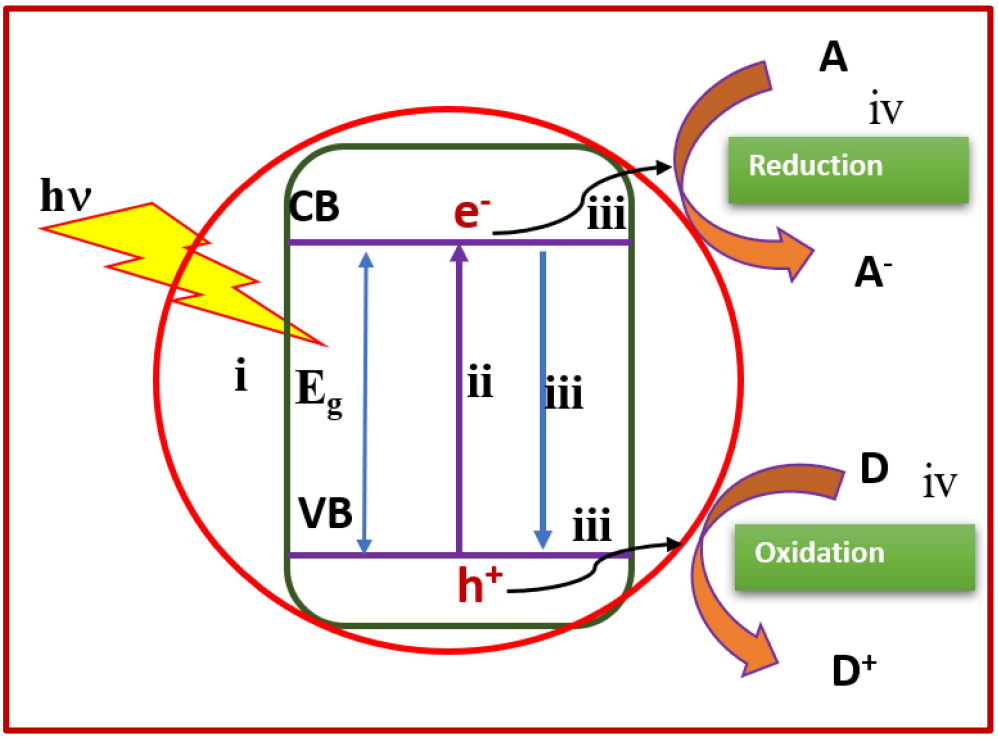

Figure 1.1 Schematic presentation of steps involved in the mechanism of the semiconductor photocatalysis.

(iv) Utilization of excited charges: The excitons on the surface of semiconductors get utilized for redox reactions. For the oxidation reaction, the redox potential of the molecule to be oxidized should be lesser than the VB of the photocatalyst. Similarly, for reduction reaction, the reduction potential of the molecule to be reduced (or the electron recipient) should have a more positive value than the CB. The difference between the band position and the redox potential of the target molecule is known as the overpotential and should be sufficiently large. The overpotential required for a given reaction can change with the photocatalyst. Whether recombination occurs or photo-excited species (holes

and electrons) react with the adsorbed molecules depends on the relative kinetics of the alternative processes.

For the effective functioning of a photocatalyst, the recombination of electron-hole should be slow or the lifetime of the separated charges should be relatively more. The ultimate objective is to increase the number of excited electrons and holes available for redox reaction without recombining. Also, the kinetics of the redox reactions at the photocatalyst surface should be faster than the typical lifetimes of separated charges.

1.3 Strategies for efficient charge separation

There are several methods which are used for improving the photocatalytic efficiency of semiconductor photocatalysts such as metal deposition, metal or non-metal doping, surface dye sensitization, and semiconductor heterostructures.

1.3.1 Metal deposition

Metal deposition on the semiconductor surface is an effective technique for improving photocatalytic efficiency [Zhang *et al.* (2019)]. Here, typically, metal nanostructures are precipitated on a parent semiconductor particulate. Since the Fermi energy level of the metal is lower than that of the semiconductor, electrons continuously move from the semiconductor to the metal until the levels become the same. The metal and semiconductor surfaces obtain excessive negative and positive charges. Hence, there is band bending near the interface where the semiconductor is in contact with the metal, thereby forming a Schottky barrier. The Schottky barrier suppresses electron-hole recombination by capturing the photogenerated electrons at the surface of the metal [Khan *et al.* (2015)]. In this way, photocatalytic efficiency gets enhanced.

1.3.2 Metal or non-metal doping

Figure 1.2 shows the schematic presentation of the effect of metal doping on semiconductor photocatalysis. It is a prevalent and efficient method for improving the photocatalytic performance of semiconductor photocatalyst. Doping by metal or non-metal creates defects in the crystal lattice of a pure phase semiconductor [Dozzi *et al.* (2013), De *et al.* (2020)]. These defects can trap electrons or holes and prevent their recombination.

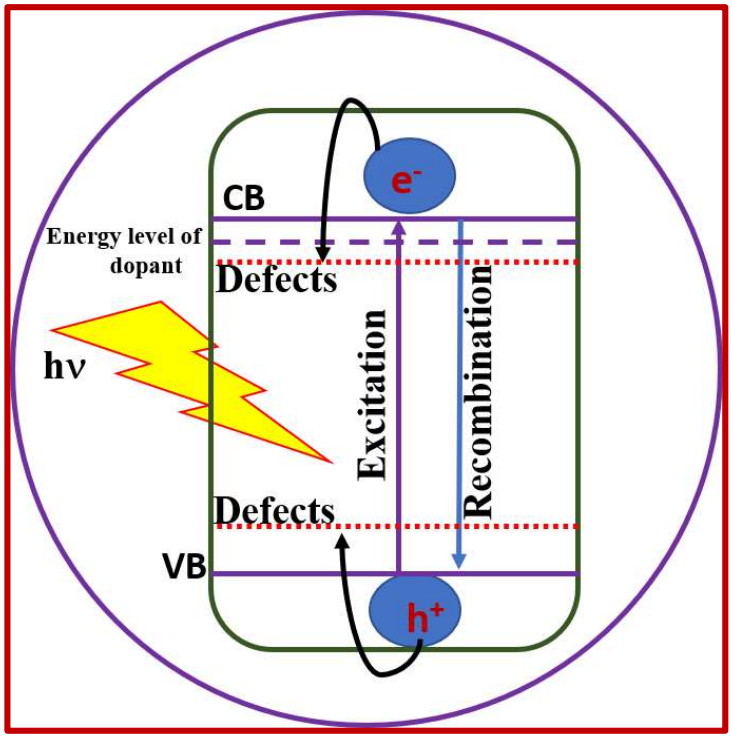

Figure 1.2 Schematic presentation of the effect of metal doping on semiconductor photocatalysis.

1.3.3 Surface dye sensitization

Dye sensitization is also an efficient method for avoiding the recombination process in semiconductor photocatalyst. Initially, it was used to modify the properties of the TiO_2 photocatalyst [O'regan *et al.* (1991)]. The organic dyes like Erythrosine B,

thionine, substituted and unsubstituted bipyridine, phthalocyanine, etc., are commonly used in the dye-sensitized process [Kamat *et al.* (1983), Ito *et al.* (2006), Chen *et al.* (2018)]. There are also some inorganic entities that have been used for surface sensitization of semiconductors. These include metal complexes such as polypyridyl complexes of ruthenium and osmium, metal porphyrin, phthalocyanine, and inorganic quantum dots [Yella *et al.* (2011), Renyal *et al.* (2011), Algar *et al.* (2014)]. Figure 1.3 shows the general photocatalytic mechanism that takes place in sensitized semiconductors subjected to irradiation by light of a suitable wavelength. If the energy of the light is greater than the HOMO-LUMO gap of the sensitizer, then in the first step the electrons are excited from its HOMO to the LUMO. Next, the electrons migrate to the CB of the semiconductor. The requirement for the operation of this mechanism is that the light used should have energy higher than the HOMO-LUMO gap of the sensitizer.

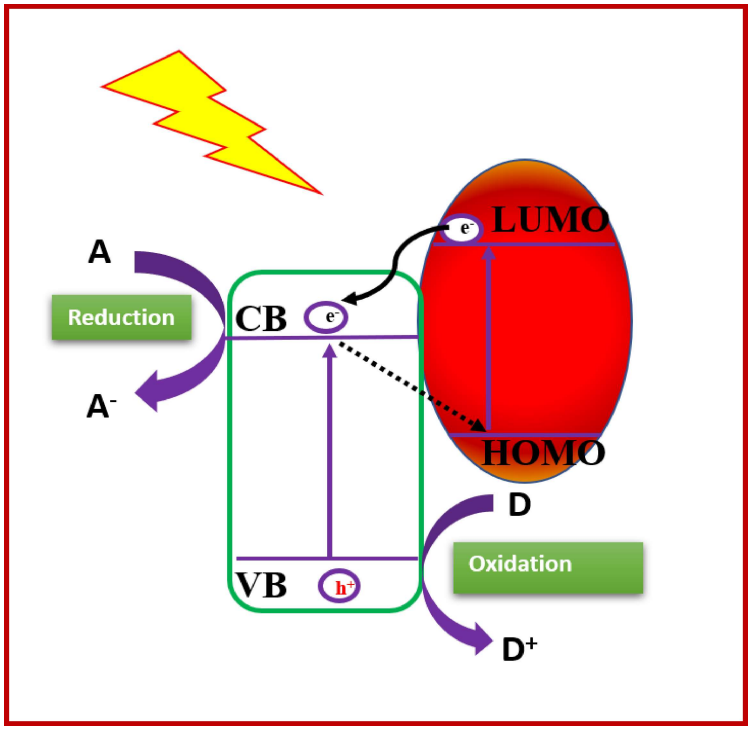

Figure 1.3 A schematic of the general mechanism of dye-sensitized semiconductor photocatalysis.

1.3.4 Semiconductor composites or heterostructures

The formation of composites having two or more semiconductors is a very efficient method of designing highly active photocatalysts. The junction formed between two semiconductors could either be a homojunction or a heterojunction. A homojunction refers to the interface between the same material but doped with either n-type or p-type (with respect to the parent material) foreign elements. For example, the n-doped (donor element) interface and p-doped (accepter element) Si semiconductors is a homojunction. If the composite involves two different phases, then they are joined together through a heterojunction. Such composites are also called heterostructures. Based on the band positions of the semiconductors, the formed semiconductor heterojunction can be classified into three types [Ge *et al.* (2019), Hu *et al.* (2017)] (shown in figure 1.4).

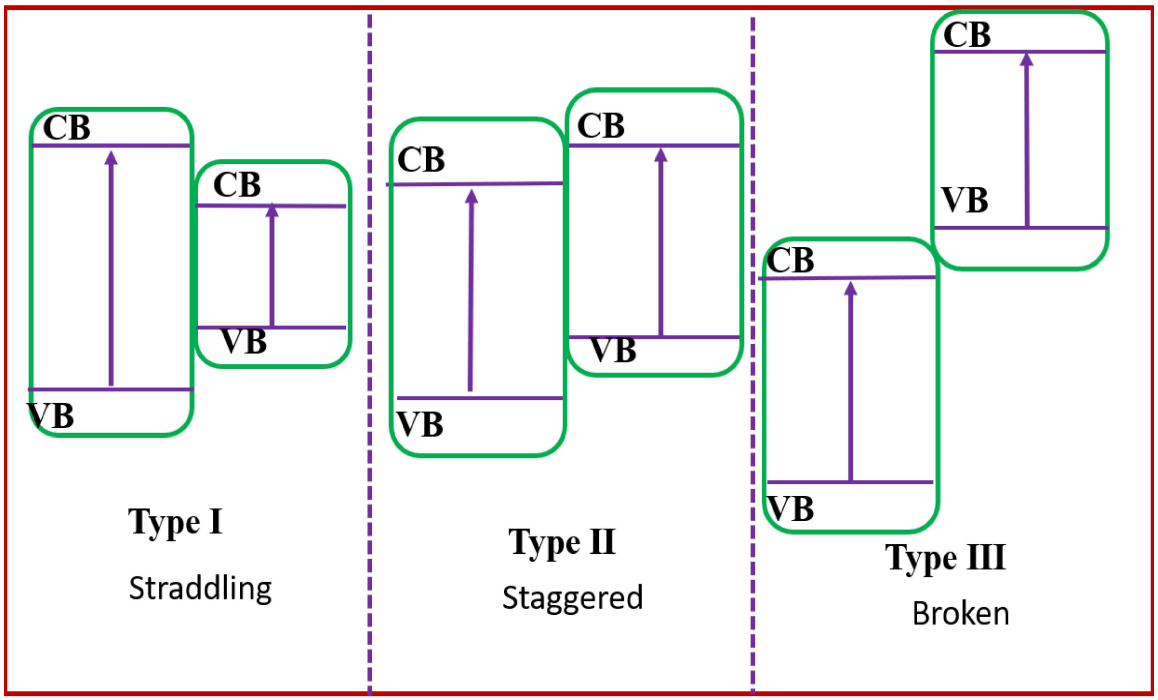

Figure 1.4 Different types of composite semiconductor photocatalyst.

In type I, i.e., the straddling type of composite semiconductor, the VB and CB edges of the semiconductor with the smaller bandgap lies between the band edges of large

bandgap semiconductor. When the type I heterostructure is irradiated with light, the excited species accumulate on the smaller bandgap part, resulting in a higher recombination rate. Contrary to this, band gaps of the two components (in the composite) do not overlap in type III heterostructures. Thus, no charge transfer can take place between the two constituent semiconductors. In this case, although the semiconductor parts are physically in contact with each other, the components act as separate semiconductor photocatalysts. Figure 1.5 shows the excitation mechanisms of type I and type III composite semiconductor photocatalysts.

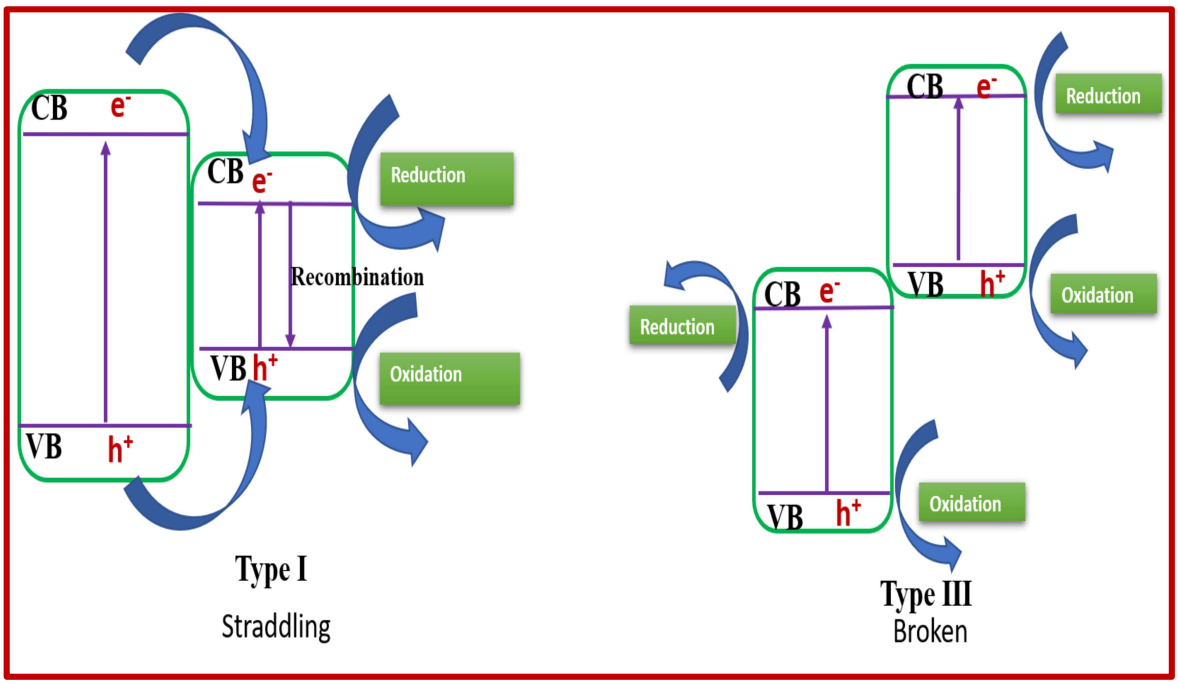

Figure 1.5 The general mechanism involved in type I and type III composite semiconductor photocatalyst.

In contrast to type I and type III, type II heterostructures shows effective charge separation (Fig. 1.5). In type II, the band edges of both components (semiconductors) are aligned in a staggered manner and two types of mechanisms are possible (shown in figure 1.6). One pathway involves a p-n junction, and the second is a Z-scheme mechanism [Low *et al.* (2017)]. The p-n junction mechanism is possible in those composites where one of

the semiconducting parts of staggered band alignment is n-type, and the other component is p-type.

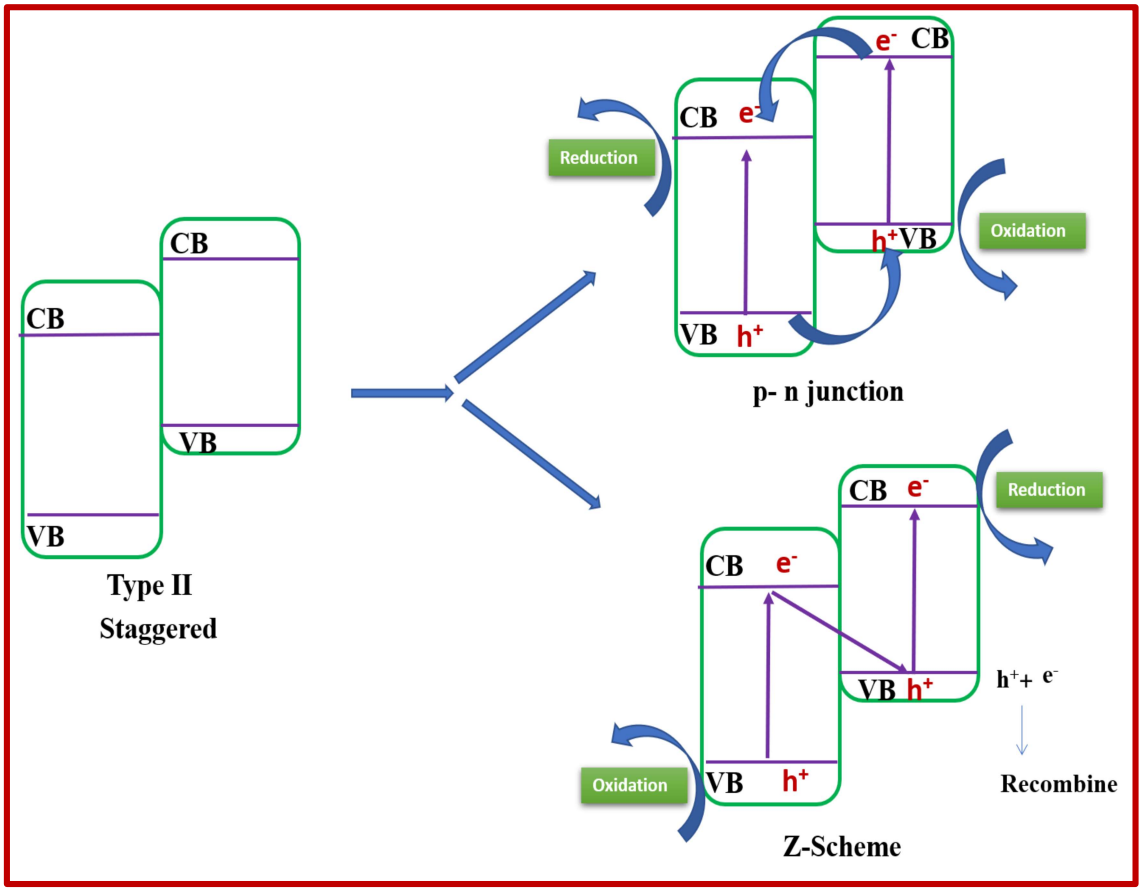

Figure 1.6 The excitation mechanism of type II composite semiconductor photocatalysts.

1.4 p-n heterojunction

An n-type semiconductor has an excess of electrons, whereas excess holes are present in a p-type semiconductor. The Fermi level (E_f) of an n-type semiconductor is nearer to its CB while the E_f is nearer to the VB position in p-type semiconductors. Thus, when an n-type semiconductor and a p-type semiconductor form a junction, the electrons on the n-type semiconductor near the p–n interface tend to diffuse into the p-type semiconductor, and the holes on the p-type semiconductor near the p–n interface tend to move to the n-type semiconductor side, leaving a charged interface (Figure 1.7 (a)). This

diffusion continues until the E_f of both components become equal. As a result, an inner electric field is generated at the interface of the p-n junction. The formation of an insulating region or depletion layer is another consequence of this phenomenon.

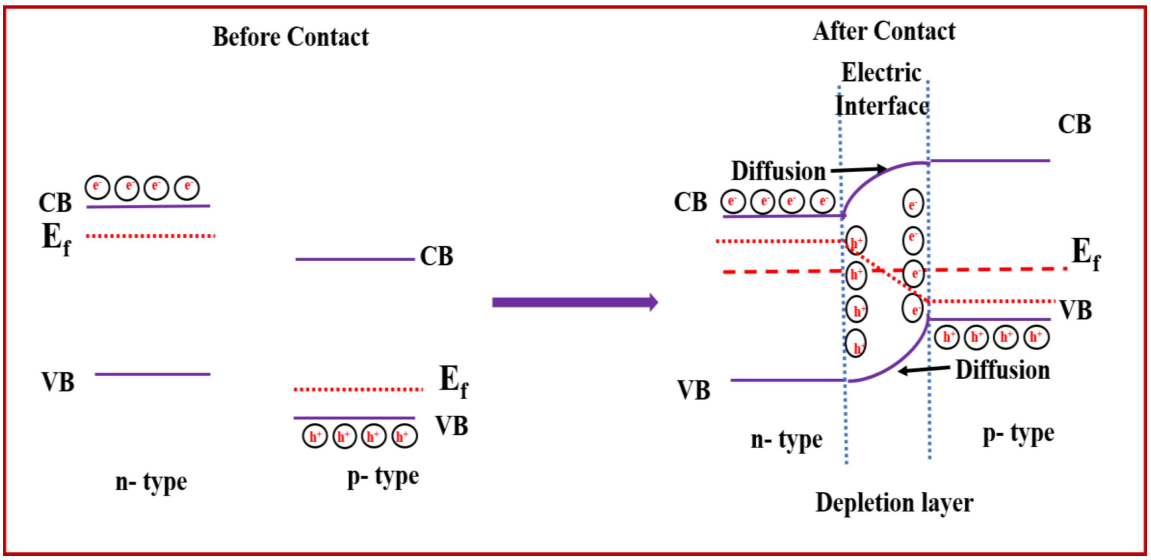

Figure 1.7 (a) Schematic representation of p-n junction formation.

When a p-n junction heterostructure is irradiated with light, both p-type and n-type components get excited, and the electron-hole pairs are generated. The internal electric field induces the transfer of photo-excited electrons in the p-type semiconductor part to the n-type component's CB. Simultaneously, the holes in the n-type component will migrate to the VB of the p-type semiconductor side in the composite. Consequently, the excited holes and the electrons are now on the different parts of the composite. The synergy between the internal electric field/depletion layer and the band alignment speeds up the electron-hole separation in p–n heterojunctions. Figure 1.7 (b) shows the mechanism of the excited species transfer in the p-n junction.

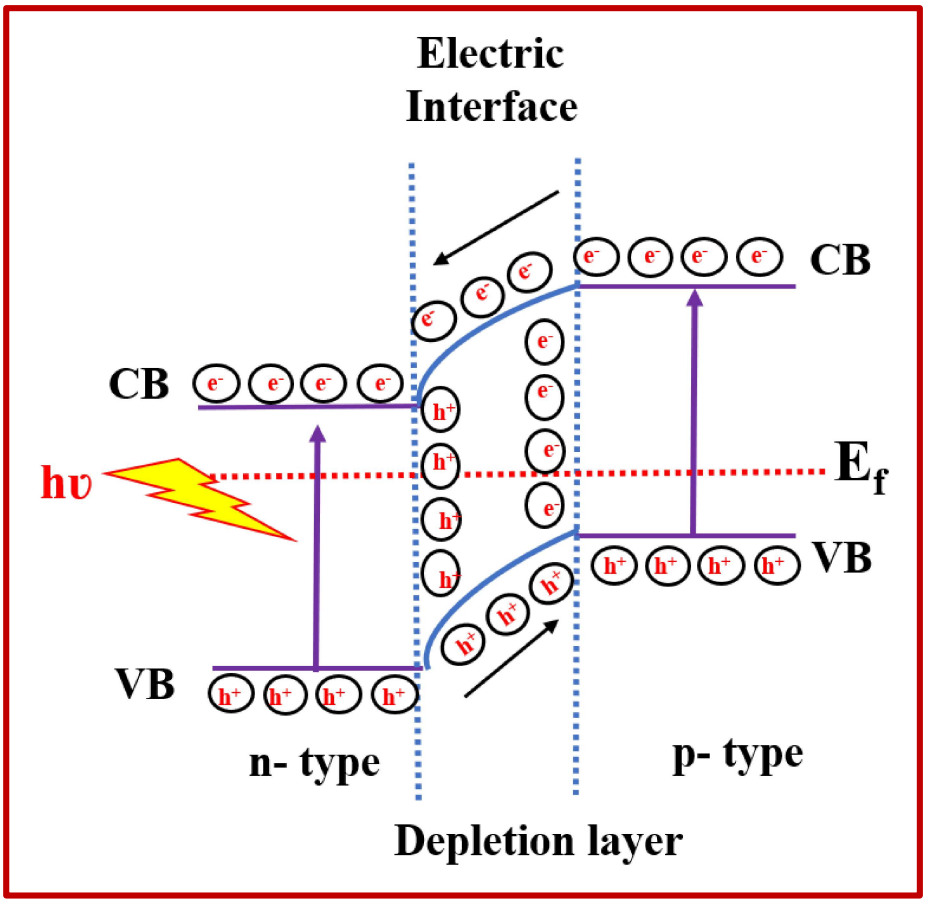

Figure 1.7 (b) Schematic illustration of the mechanism of a p–n heterojunction photocatalyst under light irradiation.

Overall, in the p-n junction photocatalytic mechanism, the photo-excited electrons migrate from the semiconductor component with higher (or less positive) CB to lower (or more positive) CB in the second component. Simultaneously, the photo-excited holes migrate from the more positive VB to the less positive VB of the other semiconductor. Therefore, the excited electrons accumulate on the lower CB side, while the holes are transferred to the semiconductor component having a higher VB position in the composite. Since the excited species are in different semiconducting parts, they are separated, and their recombination is difficult.

1.5 Z-scheme mechanism

In the Z-scheme mechanism, the photo-excited electrons in the CB of the (semiconductor) part with the lower VB edge recombine with photo-excited holes in the VB of the second part (Fig. 1.7). One can see that the internal electric field's direction in a p-n heterojunction is opposite to the electron transfer required in a Z-scheme mechanism. Thus, a Z-scheme mechanism is possible only when both semiconductor components in the composite are either n-type or p-type. The Z-scheme mechanism eventually leaves electrons on the semiconductor with the higher CB and holes on the component with the lower VB edge [Xu *et al.* (2018)]. Half of the excited species recombine in the Z-scheme mechanism; therefore, only half of the initially excited species are available for a redox reaction. But the excited species have greater overpotential than that possible in the single components.

1.6 Iron Oxides

Many semiconductors can construct such heterostructures, but iron oxide and oxyhydroxide phases are economical and have variable visible range bandgaps. Thus, these phases are likely components for the construction of efficient p-n heterojunction photocatalysts. Figure 1.8 shows the known iron oxide, hydroxide, and oxyhydroxide phases.

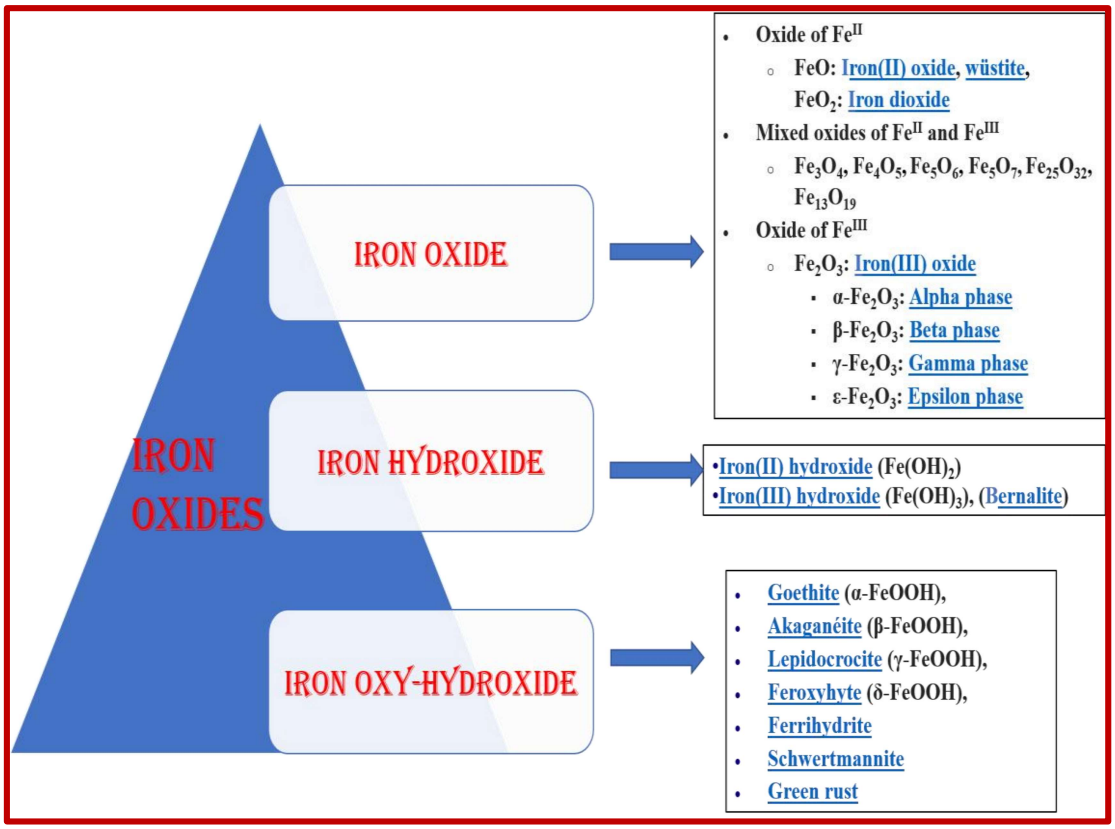

Figure1.8 Different phases of iron oxides.

The present thesis investigates magnetite (Fe_3O_4), goethite (α- FeOOH), and akageneite (β- FeOOH) phases for the synthesis of p-n heterojunction photocatalysts. These iron oxide/oxyhydroxide phases are non-expensive, have low toxicity, and biodegradable [He *et al.* (2015), Ali *et al.* (2016)]. The above properties make it more advantageous over the other nanostructure.

Fe_3O_4 is an n-type semiconductor, and in bulk, has a bandgap of only 0.1 eV. Nevertheless, on reducing particle size to nano-dimensions, the bandgap increases substantially [Liu *et al.* (2017), Radoń *et al.* (2017)]. It is magnetic, exhibits good conductivity, and readily forms heterojunctions. Magnetite acts as an electron–transfer channel and acceptor, suppressing the photogenerated carrier recombination and enhancing the photocatalytic efficiency. Cao *et al.* (2015) illustrated the visible light

activity of a composite of conductive Fe_3O_4 and AgBr. Magnetic recyclability provides a convenient way to remove the catalysts rapidly and efficiently from the reaction mixture.

FeOOH is a widely existing iron mineral in nature. The most stable phases of FeOOH are α- FeOOH and β- FeOOH [Maiti *et al.* (2015), Xu *et al.* (2015)]. α- FeOOH is an n-type semiconductor having a bandgap in the range of 2.5-3.0 eV, while nano β-FeOOH is a p-type semiconductor having a bandgap of 2.0-2.5 eV [Zhang *et al.* 2011, Prameshwari *et al.* (2011)]. He *et al.* (2002) and Wang *et al.* (2009) reports that α- FeOOH shows good photocatalytic activity in the presence of UV light. The visible-light photocatalytic activity of α- FeOOH can be further improved by structural modification using different dopants and making composites with other semiconductors. Liu *et al.* (2010) used boron-modified α- FeOOH to degrade polystyrene plastic under visible light. Similarly, Shan *et al.* (2017) used nano-goethite and graphene complex to degrade tylosin under visible light. Additionally, Wu *et al.* (2018) demonstrated the visible light activity of a composite of nano-goethite and natural organic luffa sponge to degrade rhodamine B.

Investigations have revealed that the photocatalytic activity of β-FeOOH can be enhanced by surface modification. Thus, Zhao *et al.* (2010) demonstrated the improved catalytic activity of resin-coated β-FeOOH in photo-Fenton-like processes. Recently, a DFT-based investigation [Huang *et al.* (2019)] found that β-FeOOH is more efficient than the other two FeOOH phases (α-FeOOH and γ-FeOOH) for photocatalytic water splitting under visible light. In another report, Xu *et al.* (2015) found that β- FeOOH exhibits better visible photocatalytic activity than α-FeOOH.

In general, these iron oxide and oxyhydroxide phases (Fe_3O_4, α- FeOOH, and β-FeOOH) exhibit visible light photocatalytic activity suitable for p-n heterojunction

formation. The next section illustrates various liquid phase methods for the preparation of iron oxide-based p-n heterojunction photocatalysts. Other techniques, like the solid-phase method, gas phase method, and electrospinning, have also been used to prepare heterojunction photocatalysts. The present research work mainly uses the deposition-precipitation method to synthesize iron oxide-based p-n heterojunction. Hence, the forthcoming literature survey focuses on related liquid phase synthesis procedures employed to prepare composites.

1.7 Synthesis strategies

As discussed earlier, in a p-n heterojunction, an electric field is formed near interfaces due to the diffusion of electrons and holes. The electric field created at the interface is the driving force for the spatial separation of electron-hole pairs. Thus, an enlarged contact interface gives better scope for spatial separation of the electron-hole pairs and thereby increased photocatalytic efficiency [Low *et al.* (2017)]. Further, to improve the photocatalytic performance of p-n heterojunction, the morphology should have a high surface area. Nano- heterostructures are preferred because of their high surface area. Nanosize facilitates the photogenerated electrons' movement and holes to the catalyst's surface due to minimal travel distance.

There are mainly two types of morphologies that satisfy this requirement. First is a surface decorated system, in which fine nanostructures of one semiconductor are precipitated or deposited on the surface of another. The second nanostructure is the Janus type structure. In the Janus structure, both components are comparable in size, and one semiconductor is deposited on the other's surface.

1.7.1 Deposition-Precipitation method

The process follows a stage-wise co-precipitation strategy. The first step is to prepare the nanoparticles of the major phase by precipitation. Next, the particulates are washed to remove any ions, etc., deposited on the nanostructures' surface. Then the other component is precipitated on the surface of the nanoparticles [Pakhomov *et al.* 2005]. The component to be precipitated on the nanoparticle surface is first adsorbed on its surface, and then the precipitation procedure is initiated. This method produces nanostructures with a narrow size distribution. Zhang *et al.* (2016) and Li *et al.* (2017) used deposition-precipitation methodology to prepare surface decorated heterostructures of Ag_3PO_4 /CeO_2 and Ag_2O/BiOCOOH, respectively. Similarly, Huang *et al.* (2017) fabricated Cu_2S/P25 p-n heterojunction nanostructures by the deposition-precipitation technique.

1.7.2 Hydrothermal/solvothermal method

In hydrothermal/solvothermal processes, chemical reactions are performed in sealed vessels. The temperature of solvents is raised to above their critical points via heating under high-pressure conditions [Li *et al.* (2016)]. If water is used as a solvent, then the process is referred to as the hydrothermal method. High temperature and pressures generated facilitate better solubility, faster reactant diffusion, and reaction kinetics. One can access nanostructures of different sizes and morphologies by controlling factors such as temperature, pH, reactant concentration, and additives. Extreme conditions make possible the preparation of metastable nanostructures through this route. Thus, Zhang *et al.* (2014) used a one-pot solvothermal process to construct 2D MoS_2/CdS nanohybrids. Similarly, San *et al.* (2018) reported a one-step hydrothermal method for synthesizing NiO/ZnO heterojunctions.

1.7.3 Other methods

Besides these two methods, p-n heterojunction nanostructures have also been fabricated by ion implantation, microwave, and sonochemical methods. The ion implantation method involves an exchange process that replaces particular ions in an ionic crystal. The technique requires exposing the parent ionic crystals to new ions in suitable solvent and reaction conditions. The ion exchange process takes place more quickly for nanocrystals than the bulk phase because of the former's larger surface area. Takeuchi *et al.* (2000), Yamashita *et al.* (2002), and Ghicov *et al.* (2006) demonstrated used the ion implantation technique to modify the electronic structure of TiO_2 semiconductors.

In microwave-assisted synthesis, microwave irradiation heats the reaction systems based on polar solvents quickly and uniformly. Recently, Ganapathy *et al.* (2020) demonstrated the microwave-assisted synthesis of ZnO/PbS heterojunction photocatalyst.

The sonochemical technique requires irradiating a liquid reaction system with ultrasound radiation. Such irradiation could produce extreme conditions like high temperatures, pressures, and cooling rates. Yu *et al.* (2011) reported a facile and efficient approach for the fabrication of Co_3O_4 and $CuO/BiVO_4$ composite photocatalysts via ultrasound irradiation at room temperature. The obtained photocatalyst has high crystallinity. Similarly, Kaviyarasan *et al.* (2018) reported sonochemically synthesized $Cu_2O@TiO_2$ heterojunction nanocomposites with high crystallinity.

1.8 Methods for investigating the p-n heterojunction mechanism

There are several methods to analyze the p-n heterojunction mechanism. As discussed earlier, the efficient separation of electron and hole pairs in p-n heterojunction is due to the formation of an inner electric field/ depletion layer at the interface/junction of the semiconductors. The Mott- Schottky (MS) plots are a standard electrochemical

method for finding whether a p-n heterojunction has been formed or not. A p-n heterojunction is present in the composite if the electrochemical investigation results in a "V-shaped" MS plot. MS plots also give the flat band potential value required to find the VB and the CB positions of a semiconductor. The flat band potential of an n-type semiconductor is near its CB, while the flat band potential of a p-type semiconductor is near its VB. As the p-n heterojunction formation occurs, there is shifting in the band edge positions to equilibrate Fermi level. The change in band positions is found by calculating the component semiconductors' band edges position before and after they form a p-n heterojunction.

The electron transfer kinetics of a semiconductor is studied through a Nyquist plot from the electrochemical impedance spectrum (EIS) data. The electron transfer kinetics between the component semiconductors in a heterojunction is vital for understanding the photocatalysis mechanism. An increase in the electron transfer kinetics in the composite, compared to that in the component semiconductors, points to improved charge separation due to the heterojunction formation.

1.9 Literature review of p-n heterojunction photocatalyst

The p-n heterojunction materials were first introduced by Serpone *et al.* (1984). The authors described the multi-component heterojunction photocatalyst CdS/TiO_2 system. Later, Spanhel *et al.* (1987) investigated the CdS/ZnO heterojunction. Afterward, the other researchers, Yoshimura *et al.* (1988), Gopidas *et al.* (1990), and Tian *et al.* (1996) combined CdS with different wide bandgap semiconductors to construct heterojunctions. Bedja *et al.* (1995) studied the charge transfer mechanisms in SnO_2/TiO_2 heterostructures with different structure modifications. When the two components in the SnO_2/TiO_2 heterojunction were in contact (or coupled together), the excited species got

efficiently separated. On the other hand, the encapsulation of SnO_2 in a TiO_2 shell traps one of the excited species in the core of the heterostructure, making it unavailable for a reaction. Thus, structure and morphology are vital for better photocatalytic efficiency.

The previous discussions tell us that the main structural features required for constructing an efficient p-n heterojunction photocatalyst require the optimal interfacial contact between the two components. The overall morphology should expose both semiconductors parts to light. Another vital issue is the bandgap of the component semiconductors. The visible range in the electromagnetic spectrum of solar radiation is nearly 45%. Given this, to ensure the better utilization of solar radiation, a heterostructure's semiconductor components should have bandgaps that can be excited by visible light. More of the visible range can be used for photo-excitation if semiconductors with small to moderate bandgaps (from 1.3 to 2.7 eV) are preferred for making heterostructures. Accordingly, the present thesis centers on using iron oxide and oxyhydroxide phases (with bandgaps in the 2.0-2.6 eV range) as one of the components for constructing a p-n heterojunction photocatalyst. Given this premise, the next two sub-sections present a survey of the scientific literature published on the photocatalytic investigations using iron oxides and oxyhydroxides.

1.9.1 Fe_3O_4 based p-n heterojunctions

Fe_3O_4 is a superparamagnetic and an n-type semiconductor having variable bandgap in the range of ~1.5-2.5 eV. As a superparamagnetic material, it has attracted more attraction in various fields, including ultrahigh-density magnetic recording, magnetic fluid, and biomedical materials [Ramazanov *et al.* (2017), Lahiri *et al.* (2016) and Cheng *et al.* (2005)]. While nanoparticles have several advantages, they are always difficult to separate and reuse for catalytic applications. Superparamagnetic nanoparticles get magnetized and demagnetized on application and removal of the external magnetic

field. Simple magnetic decantation can separate such nanoparticles from the reaction medium. The nanoparticles can be subsequently re-dispersed in a new reaction medium by removing the magnetic field.

Pure phase magnetite nanoparticles are not suitable for photocatalytic processes due to photo corrosion. Hence, Fe_3O_4 is coupled with other stable and photoactive materials to obtain composites with enhanced photocatalytic activities. Various researchers have reported hybrids of Fe_3O_4 nanoparticles with noble metals that not only protect it from corrosion but also improves its photocatalytic efficiency [Zhang *et al.* (2011), Mahmood *et al.* (2015), Kronkalns *et al.* (2014) and Saljooqi *et al.* (2020)].

Researchers have found Fe_3O_4 to be a promising component for p-n heterojunctions. Fe_3O_4@Fe_2O_3 heterostructures, fabricated by Wei *et al.* (2011), influenced the charge separation and changed the charge transport direction and recombination velocity. Li *et al.* (2013) prepared magnetically separable Fe_3O_4/BiOI nanostructures that degraded rhodamine B. Later, Cao *et al.* (2014) used Fe_3O_4 nanoparticles and $FeWO_4$ nanowires to synthesize a p-n heterojunction photocatalyst that effectively degraded methylene blue dye.

Similarly, Ji *et al.* (2015) prepared Ag_3O_4/Fe_3O_4/GO ternary heterostructures with enhanced photocatalytic activity. Feizpoor et al. (2018) constructed TiO_2/Fe_3O_4/$CoWO_4$ nanocomposites for removing dyes under visible light irradiation. Cao et al. (2019) recently synthesized BiOBr/Fe_3O_4 for photocatalytic degradation of the herbicide glyphosate. This photocatalyst exhibited excellent stability and reusability. Similarly, Jiang *et al.* (2019) fabricated Fe_3O_4 quantum dot modified BiOCl/$BiVO_4$ p-n heterojunction to degrade broad-spectrum antibiotics under visible light.

1.9.2 α- FeOOH based p-n heterojunction photocatalysts

There are a few studies reported on α- FeOOH based p-n heterojunction photocatalysts. Malathi *et al.* (2017) prepared rod-on-flake α-FeOOH/BiOI nanocomposite. The photocatalyst showed enhanced photocatalytic efficiency and stability. Dong *et al.* (2018) demonstrated the synthesis, and photocatalytic application of α- FeOOH modified g-C_3N_4. Similarly, Sun *et al.* (2018) reported rod-on-rod-like α-FeOOH/α-$AgVO_3$ heterostructures. The developed nanocomposite efficiently photocatalyzed the degradation of organic pollutants under visible light in an aqueous medium. Recently, Zhao *et al.* (2020) prepared amorphous α- FeOOH nanoparticles decorated graphitic carbon nitride. This heterostructure exhibited efficient photo-Fenton-like activity for degrading the antibiotic tetracycline.

1.9.3 β-FeOOH based p-n heterojunction photocatalysts

There are only limited studies on β-FeOOH based p-n heterojunction photocatalysts. Zhu *et al.* (2015) and Chowdhury *et al.* (2015) prepared β-FeOOH/TiO_2 heterostructure for different photocatalytic applications. After that, Chae *et al.* (2017) reported the synthesis of β-FeOOH/Fe_3O_4 hybrid photocatalyst. It facilitates both visible light photocatalysis and easy recovery using an external magnetic field. Later, Fang *et al.* (2018) fabricated β-FeOOH coupled with single-walled carbon nanotubes to degrade methyl orange. Recently, He *et al.* (2020) prepared metal-free g-C_3N_4 -Fe_3O_4 /β-FeOOH heterostructures for hydrogen evolution under visible light. Wang *et al.* (2020) reported in situ growth of β-FeOOH@g-C_3N_4 heterostructures. The prepared material was an efficient and stable photocatalyst for oxidizing organic contaminants under solar light irradiation by activating peroxymonosulfate.

1.10 Objectives of the thesis

The detailed literature survey given in the preceding sections shows that there have been a few investigations related to iron oxide-based p-n heterojunctions. Furthermore, the use of iron oxide phases to fabricate p-n heterojunctions with Ag/Ag_2O, Cu_2O is virtually unexplored. Therefore, this thesis deals with the synthesis of starch functionalized $Fe_3O_4/Ag/Ag_2O$, Fe_3O_4/Cu_2O, α-FeOOH/β-FeOOH, and α-FeOOH/β-FeOOH/Cu_2O p-n heterojunction photocatalysts. These heterostructures were then characterized by X-ray diffraction (XRD), Fourier transforms infrared (FTIR) spectroscopy, Transmission electron microscopy (TEM), magnetic property measurement system (MPMS), and X-ray photoelectron spectroscopy (XPS). Solid-state UV-visible diffuse reflectance spectroscopy was used for bandgap determination. The electrochemical studies were done in an electrochemical workstation/ analyzer.

The thesis then evaluates the visible light photocatalytic activities of the prepared nanostructures for different photocatalytic applications. In the first chapter, the prepared nanocomposites were used for the photocatalytic production of H_2O_2. The other chapters describe the photo-Fenton degradation of *p*-nitrophenol (PNP) and methyl orange (MO) by prepared nanostructures. A systematic approach has been adopted to investigate the mechanism and kinetics of photocatalytic degradation. The pointwise objectives of the thesis are given below.

(1) Synthesis and photocatalytic application of magnetically recyclable starch functionalized $Fe_3O_4/Ag/Ag_2O$ nanostructures.

(2) Synthesis and photocatalytic applications of magnetically recyclable starch functionalized Fe_3O_4/Cu_2O nanostructures.

(3) Synthesis and photocatalytic applications of starch functionalized α-FeOOH/β-FeOOH nanocomposites.

(4) Synthesis and photocatalytic applications of starch functionalized α-FeOOH/β-FeOOH /Cu_2O nanostructures.

The photocatalytic production of H_2O_2 and photo-Fenton degradation of p-nitrophenol (PNP) and methyl orange (MO) have been chosen to check the prepared nanocomposites' photocatalytic efficiency. The next section describes the experiments performed to check the photocatalytic efficiency.

1.10.1 Photocatalytic production of H_2O_2

H_2O_2 is a potent, green oxidizing agent with only water and oxygen as its byproducts. It has various applications as a bleaching agent in the pulp/paper/textile industry, as an oxidizing agent in wastewater treatment, as a reagent for manufacturing many inorganic and organic compounds, as a hydrogen storage medium, and energy storage chemical for hydrogen fuel cell and as a mild disinfectant. Therefore its production becomes more important. H_2O_2 is mainly produced by the anthraquinone process, direct synthesis, and photocatalytic process. Anthraquinone involves complex sequential hydrogenation and oxidation of anthraquinones in organic solvents. This process requires a significant amount of energy, chemicals and is accompanied by waste generation as well.

In contrast, the direct synthesis of H_2O_2 requires an expensive catalyst. A high amount of energy is released in this process. Therefore there is an increased risk of explosion [Henkal *et al.* (1914), Flaherty *et al.* (2018)]. In contrast to the above, photocatalytic production of H_2O_2 is a green and economical process. Photocatalytic production of H_2O_2 is carried out either by oxygen reduction or by water oxidation. O_2 by two-electron reduction gives H_2O_2. This reaction happens at 0.68 eV versus NHE. For this conduction band of the catalyst should be above the 0.68 eV. The standard potential for oxidation of H_2O is 1.23eV.

$$O_2 + 2e^- + 2H^+ \longrightarrow H_2O_2$$

$$H_2O + 2h^+ \longrightarrow 1/2\ O_2 + 2H^+$$

Chapter one presents the facile synthesis of starch functionalized $Fe_3O_4/Ag/Ag_2O$ catalyst for photochemical production of H_2O_2 using only water.

1.10.2 Photo- Fenton degradation of PNP and MO

PNP is a priority water pollutant. It has a characteristic absorption peak at 317 nm in the acidic medium and 399nm in the basic medium due to the formation of phenolate ion. MO is a water-soluble azo dye (commonly known as a pH indicator) extensively used in several industries, including the textile, paper, printing, and food industries, and mostly discharges from industrial wastewater. MO has a characteristic absorption peak due to azo linkage at 506 nm in the acidic medium and at 464nm in the basic medium. The change in the intensity of the characteristic peak (depending on the pH) with time enables tracking the progress of pollutants degradation reaction.

The photo-Fenton degradation involves the activation of H_2O_2 by oxidation of photoproduced Fe^{2+} ions. The iron oxide or oxyhydroxide based heterogeneous photocatalysts in the present thesis also display photo-Fenton activity in the presence of H_2O_2 under the visible light. The H_2O_2 breaks into hydroxyl radical ($OH^{\cdot}$), peroxide radical ($OOH^{\cdot}$), and hydroxide ion (OH^-) by different means.

$$SC + h\nu \longrightarrow SC(e^-_{CB} + h^+_{VB})$$

$$SC(e^-_{CB}) + Fe^{3+} \longrightarrow Fe^{2+}$$

$$SC(e^-_{CB}) + H_2O_2 \longrightarrow OH^{\cdot} + OH^-$$

$$Fe^{2+} + H_2O_2 \longrightarrow Fe^{3+} + OH^{\cdot}$$

$$SC(h^+_{VB}) + H_2O_2 \longrightarrow OOH^{\cdot}$$

The peroxide radical further reacts with H_2O_2 to produces $OH^{\cdot}$. Likewise, OH^- oxidized by holes and produces $OH^{\cdot}$. The $OH^{\cdot}$ has strong oxidizing power and degrades the pollutants into smaller organic molecules. The disappearance of all peaks in the spectrum indicates nearly complete mineralization or degradation of PNP and MO to smaller molecules with no UV-visible signature. The Fe^{3+}/ Fe^{2+} interconversion cycle makes catalyst more efficient and recyclable. In this process, more electrons were consumed rather than recombining with holes.